Tellus (1997), 49B, 343–356
Printed in UK – all rights reserved

TELLUS
ISSN 0280–6509

The effect of fractional cloudiness on the oxidation of SO_2

By JAN MATTHIJSEN*, KARSTEN SUHRE, PETER BECHTOLD and ROBERT ROSSET,
Laboratoire d'Aérologie, O. M. P., UMR CNRS/UPS 5560, 14, Avenue Edouard Belin, 31400, Toulouse, France

(Manuscript received 19 April 1996; in final form 12 March 1997)

ABSTRACT

We have investigated the effect of fractional cloudiness on the oxidation of SO_2 in the marine boundary layer. We address the question to which extent the budget of SO_2 is affected by the way cloudwater content and cloudcover are resolved in mesoscale meteorological models. In these models, the cloudwater and cloud cover are calculated simply from the grid-cell average temperature and total water content (all-or-nothing), or, mostly, a subgrid parameterization (fractional cloudiness) is used. Such a subgrid parameterization is considered much more realistic, but does not allow for a direct implementation of cloud chemistry. For both approaches, we have simulated the SO_2 concentration with a two-layer model, which contains the basic production and loss mechanism of SO_2 in a cloudy marine boundary layer. We found that the SO_2 concentration calculated using the subgrid parameterization to calculate the cloud parameters may deviate up to a factor of two as compared to that calculated using an all-or-nothing cloud parameterization. Calculations performed in a similar way for 5 observed cases of fractional cloudiness show maximum deviations between -85% and $+33\%$. These observed cases have been selected from the GATE, Puerto Rico '72, ASTEX, FIRE and Semamphore measurement campaigns. Meteorological chemical mesoscale models which can take fractional cloudiness into account in the simulation of cloud chemistry are expected to give an important improvement of the quantification of the sulfur budget. Consequently, the results of meteorological mesoscale models which treat SO_2 aqueous phase chemistry with all-or-nothing cloud parameters should be treated with care. Moreover, we conclude that fractional cloudiness can have a major effect on the oxidation of SO_2 in the MBL even for a relatively small cloud cover. Parameters critical to the effect are the over-all lifetime of SO_2 in the cloud and the rate of exchange between cloudy and non-cloudy air.

1. Introduction

The oxidation of DMS via SO_2 to sulfate in the marine boundary layer (MBL) contributes to the tropospheric burden of sulfate aerosols (Andreae and Raemdonck, 1983, Nguyen et al., 1983). The amount of sulfate aerosols has a direct impact on the radiative transfer. Indirectly sulfate aerosols affect the radiation budget through their influence on the albedo of clouds as they act as cloud condensation nuclei. For studies on the impact of aerosols on climate, it is therefore important to have a good understanding of the different production and loss pathways of SO_2.

In the MBL, SO_2 is produced in the gas-phase oxidation reaction of dimethylsulfide (DMS) with the hydroxyl radical (OH). Furthermore, long-range transport from continental sources may contribute to the SO_2 concentration in the MBL. The fate of SO_2 is determined by several different loss processes. Under non-cloudy conditions, the chemical loss of SO_2 is governed by oxidation to sulfate in the gas phase initiated by reaction with OH (Calvert and Stockwell, 1984). Furthermore,

* Corresponding author.

SO_2 is removed by heterogeneous loss reactions or dry deposition on sea spray and dry deposition to the sea surface (Sievering et al., 1992). Under cloudy conditions, the oxidation of SO_2 in cloud droplets can be much faster than the loss pathways mentioned above (Daum, 1990). The presence and amount of cloudwater are therefore important factors to the local SO_2 concentration and sulfate formation. The oxidation efficiency of cloudy air can be further enhanced when the transport of air through a cloud increases. Therefore, even small scattered boundary layer clouds may significantly affect the fate of SO_2.

MBL cloud types range from solid stratocumulus, which often form over cold ocean currents, to scattered cumulus clouds, which are prominent in the tradewind region. The relative importance of fractional cloudiness (FC) conditions is indicated by cloud climatologic data for cumulus (cu) and stratus and stratocumulus clouds (st/sc) over the oceans (Hahn et al., 1982; Warren et al., 1988). The average ocean cloud cover is approximately 65%. The frequency-of-occurrence for cu and st/sc are found of approximately 33% and 45%, respectively. Moreover, an averaged amount-when-present is shown for cu and st/sc clouds of 38% and 73%, respectively. For both cloud types the value for the amount-when-present suggests occurrences of FC conditions. Furthermore, cloud cover has been measured during several measurement campaigns (e.g. Cahalan et al., 1995 and Albrecht et al., 1995). They found on average FC varying from 0.26 to about 0.85 during the FIRE and ASTEX field campaigns (both campaigns are referenced later on). Moreover Chang and Coakley (1993) derive from satellite observations that the frequency of FC pixels is approximately symmetric around the maximum at a FC cover of 0.5. This indicates that a cloud cover of 0.5 is the most likely value for FC conditions.

Given the atmospheric abundance of FC conditions and their expected importance to SO_2, model studies of the SO_2 budget should take these conditions properly into account. So far, however, the effect of fractional cloud cover on SO_2 has not gotten much attention. At present, a new generation of mesoscale models is under construction, which can describe both dynamical meteorological and gas- and aqueous-phase chemical processes. With these models we will be able to simulate the distribution of sulfur species and study the governing processes in more detail than with global models. In addition this new generation of mesoscale models has the advantage over the earlier generation that the meteorology and chemistry are directly coupled. In the earlier models meteorology and chemistry are basically decoupled. These models consist in general of an Eulerian chemical transport and dispersion module which is driven by meteorological information derived from synoptic scale numerical weather-prediction models. The decoupling between every update interval has proven to cause considerable errors in the spatial and temporal development of species especially of those in the aqueous phase (Müller et al., 1996).

Mesoscale models are not cloud-resolving and apply therefore usually a FC parameterization to predict the amount of cloudwater and cloud cover under FC conditions. However, the available mesoscale FC parameterizations do not render the information which allows the description of the gas- and aqueous-phase chemistry under FC conditions. Without such a subgrid parameterization gas- and aqueous-phase chemistry can be easily described. In that case a grid cell has a cloud cover of either 1 or 0, and the amount of cloudwater is simply calculated from the difference between the total water content and the saturation mixing ratio. But models with this, so called, all-or-nothing approach (AON) do not properly account for fractional cloudiness conditions. As a consequence, the calculated amount of SO_2 oxidized may then be seriously biased.

Previously, numerous model studies have been performed in order to quantify the oxidation pathways of sulfur mainly in relation to the problem of acid deposition. Where they all highlight in this respect the importance of clouds none of them reports simulations with a fully coupled mesoscale meteorology and chemistry model which takes fractional cloudiness into account. A study by Karamchandani and Venkatram (1992) who use, however, a decoupled model shows nevertheless an important improvement of the results when taking (fractional) clouds into account. A study with a similar model (McHenry and Dennis, 1994) shows the importance of fractional cloudiness although they report the need for a better calculation of cloud fraction and cloud volume. Berge (1993) uses a coupled meteorology and chemistry model. Although he does not take

fractional cloudiness into account he suggests that including subgrid processes may be of considerable importance to the results.

In this paper we present a study of the effects of fractional cloudiness on SO_2 in the marine boundary layer (MBL). We investigate the difference between SO_2 budget calculated in a MBL with an AON approach and with a more realistic FC approach for a range of the critical FC parameters. In this way we address the question to what extent the AON approach may be used in the simulation of the SO_2 budget, and when the AON approach is expected to be inappropriate. Therefore, we have simulated the SO_2 concentrations in a MBL using a stationary state two layer model. This model describes the basic production and loss mechanisms of SO_2. In order to find the difference between the SO_2 concentration and formation in an AON or an FC approach we have calculated its steady state concentration in a MBL by using, either an AON scheme or an FC scheme to calculate the cloudwater content (q_l) and the cloud cover (N). This part of the study treats the oxidation efficiency of clouds for SO_2 under different meteorological and chemical conditions. Furthermore, we have estimated for five specific cases of fractional cloudiness the effect of using either FC or AON cloud parameters on the concentrations and the rates of the different loss pathways of SO_2. These specific cases have been selected from measurement campaigns. We treat the sensitivity of all our results to the exchange rate between cloudy and non-cloudy air and to the in-cloud oxidation rate of SO_2.

2. Description of the FC and AON cloud parameterizations

Different numerical schemes exist to describe cloud cover and cloudwater content in a typical mesoscale model (see Mocko and Cotton, 1995 for an overview). Here, we use the scheme as described by Bechtold et al. (1992) and (1993). Their scheme has been largely tested and shown to give reasonable results in comparison with LES (Large-Eddy Simulation) results obtained by using observational data (Cuijpers and Bechtold, 1995).

The basic idea of their scheme is to suppose that the liquid water potential temperature, θ_l, and the total water content, q_w, possess a joint-normal probability-density distribution with variance σ_s. The fractional cloudwater content and the fractional cloud cover can then be calculated by integrating over the fraction of the distribution that lays above the saturation curve. Fig. 1 visualizes this concept. Each ellips around the mean variable couple $(\bar{q}_w, \bar{\theta}_l)$ signifies such a distribution with a certain variance. From the hatched area above the dashed line and within the ellips the cloud fraction is calculated. Although the pictured couple $\bar{q}_w$, $\bar{\theta}_l$ lies under the saturation curve the FC scheme still can predict a cloudwater content and cloud cover depending on the specific probability-density distribution. Note that the scheme actually uses the linear approximation $\bar{q}_{sl}$ instead of the precise saturation curve.

For a full description of the FC scheme we refer to the cited references. Here we just present the equations for the cloud cover, N_{FC}, and the layer averaged cloudwater content, $\bar{q}_{lFC}$.

$$N_{FC} = \frac{1}{2}\left(1 + \mathrm{erf}\frac{Q_1}{\sqrt{2}}\right) \tag{1}$$

where "erf" designates the traditional error-function.

$$\bar{q}_{lFC} = 2\sigma_s\left(N_{FC}Q_1 + \frac{e^{-Q_1^2/2}}{\sqrt{2\pi}}\right), \tag{2}$$

where $Q_1 = a(\bar{q}_w - \bar{q}_{sl})/2\sigma_s$, and $a = [1 + L^2/(R_v c_p T_l^2)\bar{q}_{sl}]^{-1}$ given $T_l = (\bar{T}/\bar{\theta})\bar{\theta}_l$. Further, L is the latent

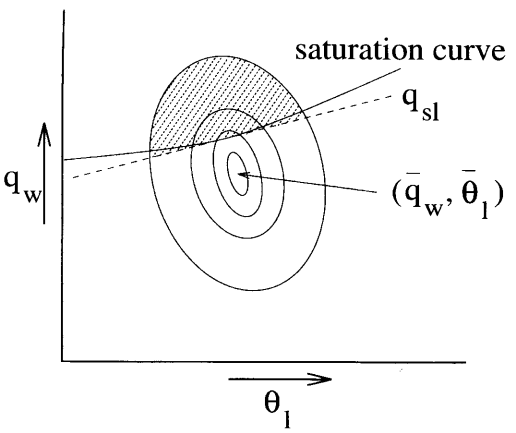

Fig. 1. Schematic graph of the FC scheme concept. Each ellips represents a joint-normal probability-density distribution of q_w and θ_l around the mean variable couple $(\bar{q}_w, \bar{\theta}_l)$.

heat of vaporization, R_v is the gas constant for water vapor and c_p is the specific heat of water vapor. The variable $\bar{q}_{sl}$ is the saturation mixing ratio at temperature T_l. Apart from the temperature and total water content it is σ_s which determines the FC parameters. The value of the variance σ_s depends on the turbulent structure of the MBL. It can be parameterized as being a function of $\bar{q}_w$ and $\bar{\theta}_l$ and the mixing- and dissipation-length (Bechtold et al., 1992). For any layer we can now calculate N_{FC} and $\bar{q}_{lFC}$, given the temperatures $\bar{T}$, $\bar{\theta}$, $\bar{\theta}_l$, the total water content, $\bar{q}_w$. The cloudwater content in the cloud is given by $q_{lFC}=\bar{q}_{lFC}/N_{FC}$. Cuijpers and Bechtold (1995) reported typical values for σ_s in the MBL ranging between $1{\cdot}10^{-5}$ and $4{\cdot}10^{-4}$. In the first part of our study, we utilize values within this range in order to calculate FC parameters for a range of possible turbulent situations. In the second part where we apply our model to five specific cases the values of σ_s are constrained by the observations.

The AON cloudwater content is calculated simply from the difference between the mean total water content, $\bar{q}_w$, and the saturation mixing ratio. In order to compare the results of the FC scheme with those of an AON scheme we calculate the AON cloud parameters using the same linearization for $\bar{q}_s$.

$$q_{lAON} = a(\bar{q}_w - \bar{q}_{sl}) \qquad (\text{for } \bar{q}_w > \bar{q}_{sl}). \tag{3}$$

Under the same conditions, the AON cloud cover, N_{AON}, is 1. For $\bar{q}_w \leqslant \bar{q}_{sl}$ both N_{AON} and q_{lAON} are equal to zero.

We have calculated the FC and AON cloud parameters assuming a homogeneous cloudy layer in the MBL with a typical temperature of 283 K. Fig. 2 shows the fractional cloud cover and the difference between the layer averaged FC and AON cloudwater content as a function of $\bar{q}_w/\bar{q}_{sl}$ and σ_s, respectively. Note that for values $\leqslant 100\%$ the fraction $\bar{q}_w/\bar{q}_{sl}$ is equal to the relative humidity in the traditional sense. In order to picture all realistic values of cloudwater content in the MBL an upper limit of 110% is large enough.

Fig. 2a shows that even for relatively small values of σ_s, a significant fractional cloud cover can be found for $\bar{q}_w/\bar{q}_{sl}$ values below 100%. The value of N_{FC} at 100% is exactly 0.5 for all values of σ_s, due to the symmetry of the applied Gaussian distribution in (1) and (2). The amount of liquid water is important to the oxidation rate of SO_2 in the cloud, as will be discussed later on. The difference between the FC and AON cloudwater content (figure 2b) is, therefore, an indication for the effect of fractional cloudiness on SO_2. As can be seen from combining (2) and (3), $\bar{q}_{lFC}-\bar{q}_{lAON}$ is always larger than zero and has a maximum when $\bar{q}_w/\bar{q}_{sl}$ is 100% of $2\sigma_s/\sqrt{2\pi}$ ($\approx 0.8\sigma_s$ (in g g^{-1})).

3. Two-layer cloud model

To simulate the SO_2 concentration in the MBL, given either the FC or AON cloudwater content and cloud cover, we use a two-layer model with a fixed cloud- and sub-cloud layer. In our model approach we assume that the SO_2 concentrations in both layers are in quasi stationary state, $d/dt\cdot\cdot = 0$. Thus the governing terms which determine the SO_2 concentration, being chemical loss and production, deposition on seaspray and sea surface and transport between cloudy and non-cloudy air are supposed to balance. This assumption restricts the applicability of our model to stationary meteorological and chemical conditions, i.e. conditions where the time scale of change of each of the mentioned processes is considerably larger than the time scale of the process itself. The contribution of long range transport to the SO_2 concentration has not been included in this study. Moreover we do not take into account entrainment of free tropospheric air. However, for our goal it is more important to maintain simplicity in the model than to explicitly quantify all possible process changes.

Fig. 3 schematically shows the processes which are taken into account to simulate SO_2: chemical loss in the gas- and aqueous phase, chemical production from the oxidation of DMS by OH, a net removal through deposition on seaspray and sea surface and transport between cloudy and non-cloudy air.

With Z_i the MBL height and Z_{cld} the lifting condensation level height, we introduce an equivalent cloud thickness (H_c) by weighting the cloud thickness with the cloud cover: $H_c = N(Z_i - Z_{cld})$. The equivalent height of the non-cloudy air is then defined by: $H_s = Z_i - H_c$.

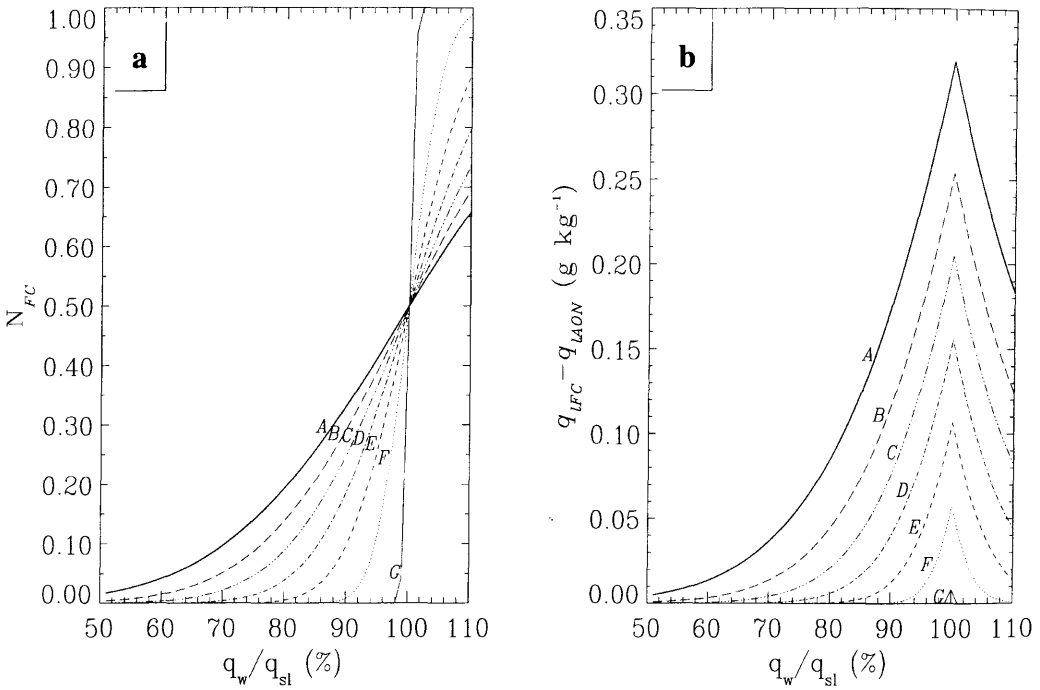

Fig. 2. Fractional cloud cover, N_{FC} (a) and $\bar{q}_{lFC} - q_{lAON}$ (b) for $T = 283$ K and for $\sigma_s = 4.0\ 10^{-4}$ (A), $\sigma_s = 3.2\ 10^{-4}$ (B), $\sigma_s = 2.6\ 10^{-4}$ (C), $\sigma_s = 1.9\ 10^{-4}$ (D), $\sigma_s = 1.3\ 10^{-4}$ (E), $\sigma_s = 7.2\ 10^{-5}$ (F) and $\sigma_s = 1.0\ 10^{-5}$ (G).

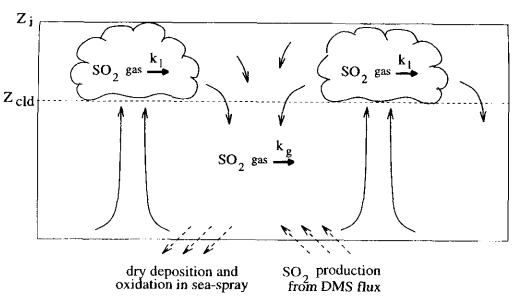

Fig. 3. Schematic view of the MBL with the SO_2 relevant processes.

3.1. SO_2 oxidation

Chemical production (P) of SO_2 in the MBL originates from the gas-phase oxidation reaction between DMS and OH (Hynes et al., 1986). In the non-cloudy air, SO_2 is only oxidized in the gas phase. The oxidation pathways of SO_2 to form sulfate includes several reactions (Calvert and Stockwell, 1984). Here we describe it by the main initial and rate limiting reaction between SO_2 and OH:

$$SO_2 + OH \xrightarrow{k_1} \text{sulfate}, \tag{4}$$

where k_1 is the reaction rate constant (molec^{-1} cm^3 s^{-1}). In cloudy air the rate of SO_2 oxidation to sulfate is much larger than in non-cloudy air due to the very efficient oxidation in the aqueous phase. The oxidation of dissolved SO_2 to sulfate in cloud droplets is a complex process of which not all aspects are well understood. Nevertheless, it has been well established that the main oxidation reactants in the aqueous phase (aq) are H_2O_2 and O_3 and to a lesser extend also OH (Jacob, 1986; Sedlak and Hoigné, 1994).

Since we do not focus here on the exact mechanism of SO_2 loss in the aqueous phase we have not explicitly included all relevant cloud-chemical reactions in the model. In order to model the loss of gaseous SO_2 in the cloudy air due to aqueous phase reactions we apply an all over quasi first-

order reaction rate constant as a function of the parameter q_l.

$$SO_2 + OH \xrightarrow{k_l(q_l)} \text{sulfate(aq)}. \quad (5)$$

Off-line, we have calculated $k_l(q_l)$ using a cloud-chemistry model with an extensive cloud-chemical mechanism (Matthijsen et al., 1995) for typical marine photochemical conditions. Marine cloud-water pH values are found within the wide range of 4 to 7 (e.g. Warneck, 1988).

Fig. 4 shows calculated values of k_l as a function of q_l for different pH conditions. The base function for k_l is formed by hourly averaged values which have been calculated for cloudwater with a pH of 5.5. The upper-limit values (high) and the lower-limit values (low) have been calculated for cloud-water with a pH of 6 and 4.5, respectively. Both extreme values are rather unlikely to be found. Nevertheless, we acknowledge that still k_l may be smaller or larger. However, rate limiting effects of aqueous-phase diffusion (Shi and Seinfeld, 1991) and non-Henry equilibrium chemistry (Twohy et al., 1989) prevent that k_l will be considerably larger than 10^{-2} s^{-1}. Furthermore, upper-limit values of k_l can only be found in very clean areas with background SO_2 concentrations of less than 5 pptv. When more SO_2 is present the average cloudwater pH will drop very fast to values of 5.5 or less which leads consequently to a decrease of k_l. Similarly the lower-limit values will be found under rather polluted conditions involving for oceanic areas unusually high SO_2 concentrations. The following initial ambient concentrations have been used to calculate k_l: $O_3 = 30$ ppbv, $H_2O_2 =$ 0.2 ppbv and OH $= 1.0 \cdot 10^6$ molec cm^{-3}. The k_l values compare well with rates calculated for similar conditions as shown by, e.g., Iribarne and Cho (1989), and Schwartz (1994). The values of k_l were found to be insensitive to SO_2 concentrations in the typical marine range from 0 to 150 pptv. For a cloudwater content of zero the values of k_l are set equal to the quasi first-order reaction rate constant in the gas phase, $k_l \times$ [OH]. When q_l increases the value of k_l increases as well depending on the pH.

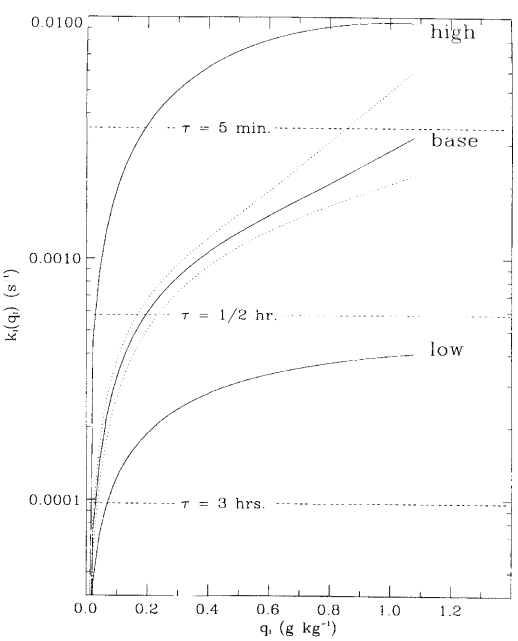

Fig. 4. Quasi first-order reaction rate constants, k_l, for the in-cloud oxidation of SO_2 as a function of the cloud-water content, q_l. Hourly average (solid lines) for different cloudwater pH (see text): a lower-limit (low), a base case (base) and the upper-limit (high). For the base case the dashed lines indicate the 10-minute average: at the beginning of a cloud (below) and at the end of a cloud (above). The chemical lifetime of SO_2 in the cloud, τ, is indicated.

In the sub-cloud layer we parameterize the removal of SO_2 caused by dry deposition on sea spray and the sea surface and by heterogeneous reactions on sea spray with an overall deposition velocity v_d. We assume a typical deposition velocity for SO_2 of 1 cm s^{-1} based on Sievering et al., (1989) and Suhre and Rosset, (1994).

The exchange rate between the cloudy and non-cloudy air will be important to the oxidation efficiency, since SO_2 is much faster oxidized in the cloud than outside. We describe the transport of air between the cloudy and non-cloudy layer following the approach of Lelieveld and Crutzen (1990) and (1991). They define a residence time, t_{cld}, of air inside a cloud by:

$$t_{cld} = \frac{H_{cld}}{w_{up}} \quad (6)$$

where w_{up} is the updraft velocity at cloud base and H_{cld} is the cloudthickness $Z_i - Z_{cld}$. By applying this vertical advective time scale, we describe the exchange between the cloudy and non-cloudy air. The assumption of a stationary cloud field leads to a time scale of t_{cld}/f for the sub-cloud layer, where f is the fraction H_c/H_s. This way of

modeling allows us to describe the transport between the two layers without describing in detail the MBL dynamics. The magnitude of t_{cld} found for clouds in the MBL has a wide range and depends on the specific meteorological conditions. Krueger et al. (1995) simulates the stratus-to-cumulus transition in the MBL. They calculate updraft- and downdraft velocities which range from a few cm s^{-1} up to 3 m s^{-1}. Given an average cloud thickness of 500 m and the definition (6) the residence time ranges from several hours to a few minutes. In our calculations we apply three different values for t_{cld}; 3 h, 30 min and 5 min. It should be noted that the value of t_{cld} is probably not independent of the variance σ_s, since the updraft velocity at cloud base is clearly linked to the turbulent structure in the MBL. However, in the context of this simplified modeling approach σ_s and t_{cld} have been varied independently rather than parameterizing a dependency between the two parameters.

3.2. *Model equations*

Combining the above mentioned processes the following equations then determine the SO_2 concentrations in the cloud (IC) and outside the cloud (OC). Note that by using the fraction f the cloud cover is implicitly introduced into the equations.

$$\frac{d}{dt}[SO_2]^{IC} = -\left[k_l(q_l) + \frac{1}{t_{cld}}\right][SO_2]^{IC} + \frac{1}{t_{cld}}[SO_2]^{OC} + P, \quad (7)$$

$$\frac{d}{dt}[SO_2]^{OC} = -\left[k_g + \frac{v_d}{H_s} + \frac{f}{t_{cld}}\right][SO_2]^{OC} + \frac{f}{t_{cld}}[SO_2]^{IC} + P. \quad (8)$$

For stationary meteorological and chemical conditions, $d/dt = 0$, $[SO_2]^{IC}$ and $[SO_2]^{OC}$ can be calculated as follows:

$$[SO_2]^{IC} = P\frac{\varepsilon[k_g + v_d/H_s]/k_l(q_l) + (1+f)}{[\varepsilon+1][k_g + v_d/H_s] + k_l(q_l)f}, \quad (9)$$

$$[SO_2]^{OC} = P\frac{\varepsilon + (1+f)}{[\varepsilon+1][k_g + v_d/H_s] + k_l(q_l)f}, \quad (10)$$

where the dimensionless number ε is the fraction between the time scale of exchange and the chemical lifetime of SO_2 in the cloud ($\varepsilon = t_{cld}/\tau$). The value of τ is defined by $1/k_l$. The value of ε signifies the different oxidation efficiencies of the (fractional) cloudy MBL. Basically three different regimes may be classified based on the value of ε: $\varepsilon \gg 1$, $\varepsilon \approx 1$ and $\varepsilon \ll 1$, respectively. For $\varepsilon \gg 1$ the time scale of exchange of air between the cloudy and non-cloudy air is much larger compared to the time scale of in-cloud oxidation of SO_2. Transport is in that case the limiting factor for the amount of SO_2 oxidized in the cloud. Similarly, for $\varepsilon \ll 1$, cloud chemistry is that slow as compared to the transport that it will be the limiting factor for the amount of SO_2 oxidized by the cloud. In the case that $\varepsilon \approx 1$ the oxidizing capacity of the cloud for SO_2 is most efficient.

In the next section we present results of the 2-layer model based on FC and AON cloud parameters, q_l and N which are calculated as a function of the total water content, q_w and the variance σ_s for different values of t_{cld} and k_l. The model runs have been performed assuming fixed cloud boundaries and temperature (see table 1). Moreover only warm MBL clouds are considered. Table 1 shows the model parameters which are used.

4. Results

In the first part of this section, we show the possible differences between the amount of SO_2 oxidized in a "FC" or an "AON" MBL which are expressed by ΔSO_2. ΔSO_2 is the difference between the SO_2 concentration integrated over the MBL for the FC and the AON case relative to the integrated AON concentration. When ΔSO_2 is smaller (larger) than zero the total SO_{2FC} concentration is smaller (larger) than the total SO_{2AON} concentration. This means that when ΔSO_2 is smaller (larger) than zero the FC scheme renders the MBL a more (less) efficient oxidizer for SO_2. ΔSO_2 is essentially independent of P, due to our assumption that P is the same in- and outside the cloud. This assumption is based on the fact that the product of [DMS] and [OH] is more or less constant in the MBL. A test showed that the results were not sensitive to this assumption. An increased or decreased SO_2 production by 50% inside the cloud compared to the production outside the cloud made virtually no difference for ΔSO_2 in those cases where the AON scheme

Table 1. *Model parameters*

Parameter	Comment/ref.	Value
Z_i	cloud top	750 m
Z_{cld}	cloud base	500 m
$[OH]$	diurnal average, marine (Thompson, 1995)	$1.0 \cdot 10^6$ molec cm^{-3}
$[DMS]$	40–140 pptv (ASTEX/MAGE-1992)	100 pptv
pH	for k_1, see text	4.5, 5.5, 6.0
$[O_3]$	for k_1, see text	30 ppbv
$[H_2O_2]$	for k_1, see text	0.2 ppbv
k_1	Atkinson (1984)	1.1 10^{-12} molec^{-1} cm^3 s^{-1}
k_2	Hynes et al. (1986)	6.14 10^{-12} molec^{-1} cm^3 s^{-1}
k_g	$=k_1 \times$ [OH]	1.1 10^{-6} s^{-1}
P	$=k_2 \times$ [DMS][OH]	1.54 10^4 molec cm^{-3} s^{-1}
T	temperature at cloud level	283 K
v_d	see text	1.0 cm s^{-1}
t_{cld}	see text	3 h, 30 min, 5 min
k_l	function of q_l	$1.1 \cdot 10^{-6}$–$1.0 \cdot 10^{-2}$ s^{-1}
σ_s	applied range	$1.0 \cdot 10^{-5}$–$4.0 \cdot 10^{-4}$

predicted no clouds. For the cases that the AON scheme did predict clouds the values of ΔSO_2 were increased or decreased, respectively by not more than an extra few percent up to 10%.

In the second part we show for five specific meterological cases the effect of using either a FC or an AON scheme on the amount of SO_2 oxidized and on the different loss rates. For these five cases σ_s and q_w have a specific value which are determined by the observational data. These marine cloud cases cover the main possible cases of fractional cloudiness.

4.1. *ΔSO_2, possible values*

Fig. 5 shows ΔSO_2 as a function of the fraction $\bar{q}_w/\bar{q}_{sl}$ for different values of the variance σ_s. These two parameters are used in both the FC and the AON scheme to calculate cloud cover and cloud-water content. Each graph in Fig. 5 applies to a specific combination of k_l and t_{cld}.

In general it can be seen from Fig. 5 that the absolute value of ΔSO_2 increases when σ_s increases. Remember that σ_s is a measure for the variability of q_w and θ_l in a grid cell, and consequently of the turbulence. The effect of an increasing k_l value from low, base to high leads logically for all values of t_{cld} to enhanced values of ΔSO_2. Whereas a decreasing time scale of exchange from 3 h, 30 min to 5 min decreases ΔSO_2 more and more.

For the results where $\varepsilon \gg 1$ (Figs. 5a, b, d) the exchange between the cloudy and non-cloudy air plays a relatively small role. In that case, ΔSO_2 is mainly caused by the difference between the FC or AON amount of cloud water and cloud volume and the magnitude of k_l. For those where $\varepsilon \ll 1$ (Figs. 5f, h, i) an increased cycling of air through the cloud now renders the "FC" MBL for most values of $\bar{q}_w/\bar{q}_{sl}$ a larger oxidizer of SO_2 than the "AON" MBL. This in spite of the fact that for $\bar{q}_w/\bar{q}_{sl} > 100\%$ AON predicts a cloud cover which is 1 and thus always larger or equal to N_{FC}. Only when the oxidizing efficiency increases ($\varepsilon \approx 1$) the amount of ΔSO_2 becomes positive for $\bar{q}_w/\bar{q}_{sl} > 100\%$ (Figs. 5c, e, g).

The temperature used to calculate the cloud parameters has been kept fixed throughout the calculations. Although, the results are sensitive towards this value in the sense of absolute numbers, the nature of the results does not change. Lower (higher) temperatures lead to larger (smaller) values of $|\Delta SO_2|$. Nevertheless it should be noted that the maximum difference between the FC and AON value of q_l (at $\bar{q}_w/\bar{q}_{sl}$ is 100%) is the same for all temperatures.

4.2. *ΔSO_2, five specific cases*

So far we have examined the ΔSO_2 for possible ranges of σ_s and q_w/q_{sl}. Now we examine five specific (fractional) cloudy cases. They give an impression of those ΔSO_2 values we are likely to encounter. Furthermore, we examine the different

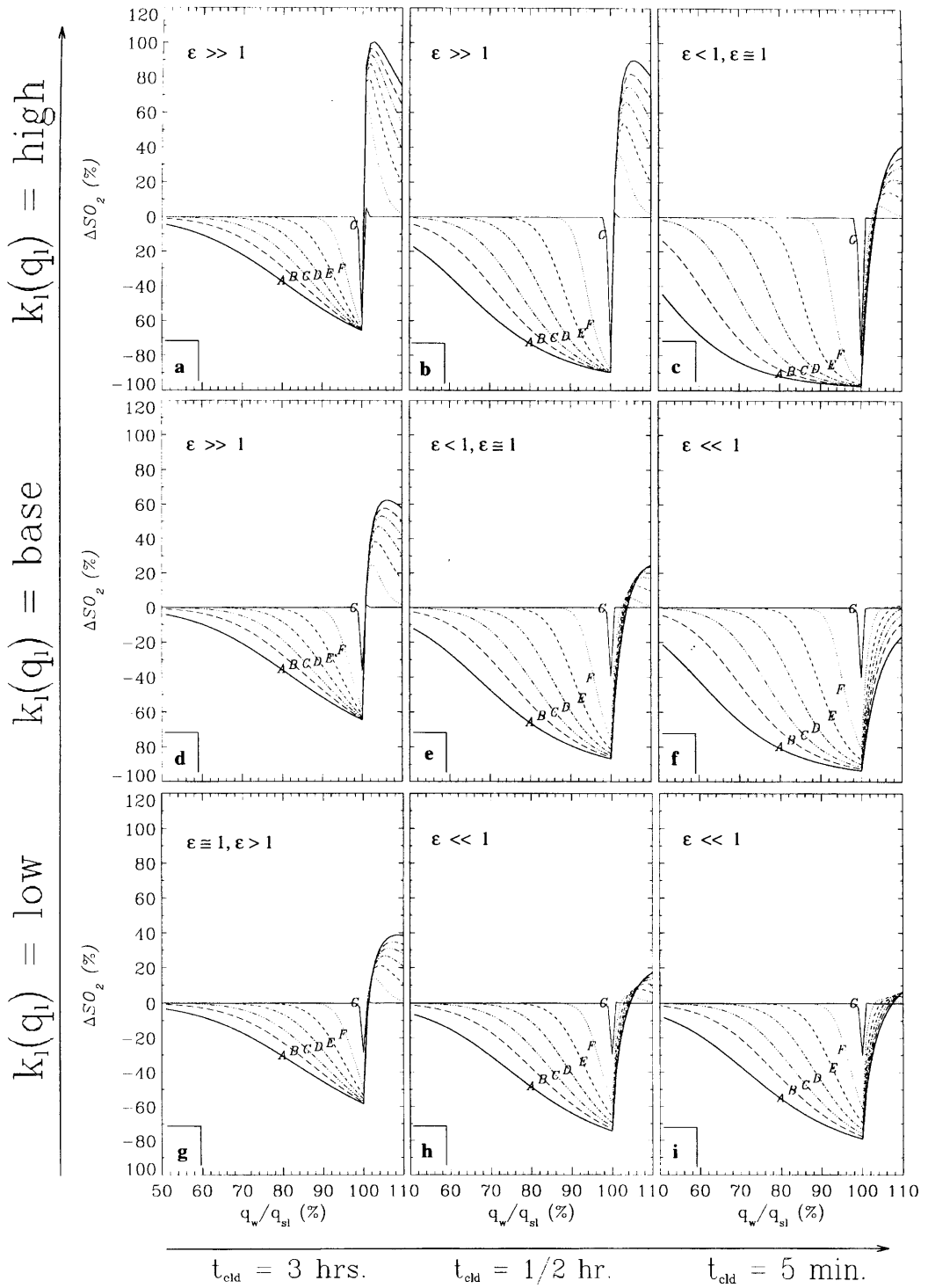

Fig. 5. ΔSO_2 (%) as a function of $\bar{q}_w/\bar{q}_{sl}$. The σ_s values (A to G) are as in Fig. 2. For the graphs from left to right as indicated along the horizontal arrow: $t_{cld} = 3$ h, 30 min, and 5 min, respectively. For the graphs from bottom to top as indicated along the vertical arrow: $k_l(q_l)$ = low, base and high, respectively. In each graph the regime is indicated by the approximate values of ε.

loss rates of SO_2, via gas- and aqueous-phase oxidation and through deposition. The choice of a FC or an AON scheme affects the magnitude of these pathways.

From the observations of five different cloud cases we have estimated the necessary cloud parameters in order to calculate the possible differences between the total SO_2 concentration in the FC and the AON approach. The observations have been gathered during the GATE (Brümmer, 1978) Puerto Rico '72 (Pennel and Lemone, 1974), ASTEX (Johnson et al., 1993), FIRE (Albrecht et al., 1988) and Semaphore (Eymard et al., 1996) measurement campaigns.

Fig. 6 indicates the general meteorological situation for the 5 different cloud cases by the profiles of q_w and θ_l. The necessary FC cloud parameters have been obtained from LES results which have been forced by the observations. This approach is similar to the one used by Cuijpers and Bechtold (1995). Table 2 gives the relevant FC and AON cloud parameters integrated over the cloud layer.

Table 3 shows the values of ΔSO_2 calculated for each of the five cases for the applied combinations of t_{cld} and k_l. The ΔSO_2 values calculated are relatively moderate in comparison with the possible maximum values, which were found for $\bar{q}_w/\bar{q}_{sl}$ is 100% (Fig. 5). In the FIRE case ΔSO_2 is mainly caused by a difference in cloud volume. ΔSO_2 lies within 16% and 33%. Changes of the value of t_{cld} and k_l are relatively small. The FC cloud volume in the ASTEX case is smaller than the AON cloud volume, whereas the opposite can be said of the cloudwater content. This leads to a ΔSO_2 which is rather sensitive to the value of t_{cld} and under fast cloud cycling conditions also to the value of k_l. The ΔSO_2 calculated range from -1% to -24%. In the GATE case the fractional cloud cover is very small ($N_{FC}=0.01$). Nevertheless the ΔSO_2 calculated are mostly of the order of 10% (from 4% to -17%). The Puerto Rico '72 case shows to be the most sensitive to the choice of the scheme. The combination of a cloud cover of 0.06 with a cloudwater content of 0.21 g kg^{-1} yield a "FC" MBL which is a larger oxidizer of SO_2 (-19% to -85%). The Semaphore case shows no difference for ΔSO_2 between the FC and AON approach, although the major loss of SO_2 occurs

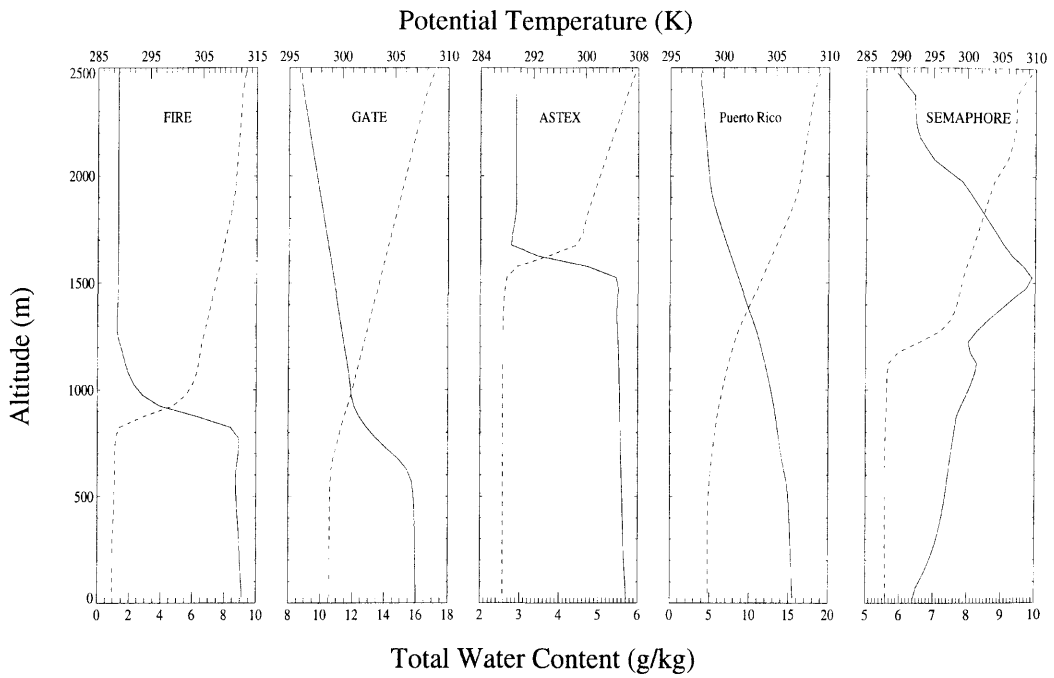

Fig. 6. Profiles of q_w (solid lines) and θ_l (dashed lines) for the five (fractional) cloud cases. Bottom scale q_w (g kg^{-1}); top scale θ_l (K).

Table 2. *FC and AON cloud parameters*

Exp.	q_l FC ($g\,kg^{-1}$)	q_l AON ($g\,kg^{-1}$)	N FC (0–1)	N AON (0/1)	Z_i FC (m)	Z_i AON (m)	H_c FC (m)	H_c AON (m)
FIRE	0.13	0.13	0.95	1	850	850	250	300
GATE	0.15	0.0	0.01	0	950	950	2.2	0
ASTEX	0.10	0.07	0.70	1	1600	1600	140	150
P.R. '72	0.21	0.0	0.06	0	1400	1400	35	0
Semaphore	0.22	0.22	1.00	1	1250	1250	300	300

Table 3. *ΔSO_2 (in %) for each case for different values of t_{cld} from left to right, and $k_l(q_l)$ from bottom to top similarly to Fig. 5*

	FIRE			ASTEX			GATE			P.R. '72			Sema.		
high	33	33	25	−2	−9	−24	4	−1	−13	−25	−61	−85	0	0	0
base	**26**	**22**	**19**	**−2**	**−5**	**−8**	**−1**	**−11**	**−17**	**−23**	**−49**	**−62**	**0**	**0**	**0**
low	19	17	16	−1	−3	−3	−2	−7	−9	−19	−32	−37	0	0	0
	3 h	1/2 h	5 m	3 h	1/2 h	5 m	3 h	1/2 h	5 m	3 h	1/2 h	5 m	3 h	1/2 h	5 m

through oxidation in the aqueous-phase (75% to 95%, see Fig. 7).

Fig. 7 shows the results for the loss rates of SO_2 for both the FC and AON scheme for the base function of k_l and the 3 different exchange time scales. In those cases where using the FC scheme instead of the AON scheme leads to significant ΔSO_2 values, the magnitude of the different loss pathways through gas-phase oxidation and deposition are clearly affected as well.

Above we have seen that the possible effects on SO_2 of using a FC scheme instead of an AON scheme to calculate N and q_l cloudwater content range between a 100% higher and a 100% lower SO_2 concentration. The magnitude depends on several parameters which determine the meteorological and chemical situation. These large discrepancies indicate that the choice of using either a FC scheme or an AON scheme in a mesoscale model is very important to the calculated amount of SO_2 and the fate of its oxidation products. Consequently, the use of a FC scheme instead of an AON scheme in mesoscale modeling of the SO_2 budget should be considered.

The frequency of occurence of cases where fractional cloudiness leads to these large discrepancies is however not expected to be as high as mentioned in the first part of this section for two reasons. First, our calculations for five observed fractional cloudiness cases show that the effect for the most likely circumstances lead to much lower ΔSO_2 values (22%, 0%, −5%, −11% and −49%). Under upper limit conditions only in one case a ΔSO_2 was found of −85%. The observed case for which we calculated these highest discrepancies is characterized by a combination of a relatively small cloud cover with a large cloud-water content. Secondly, the frequency in the real atmosphere of the meteorological and chemical conditions favourable for large discrepancies are naturally small. These conditions are large values of σ_s, small timescale of exchange (t_{cld}) and fast cloud chemistry (k_l).

5. Conclusions

We have shown with simple stationary two-layer model simulations that the amount of SO_2 oxidized in the MBL can be considerably affected by the way cloudwater content and cloud-cover are parameterized in meteorological chemical mesoscale models. The parameterization of cloud parameters in these models consists of either a fractional cloudiness or an all-or-nothing scheme. At present only the AON approach makes a direct implementation of gas- and aqueous-phase chemistry possible. Our results show that SO_2 concen-

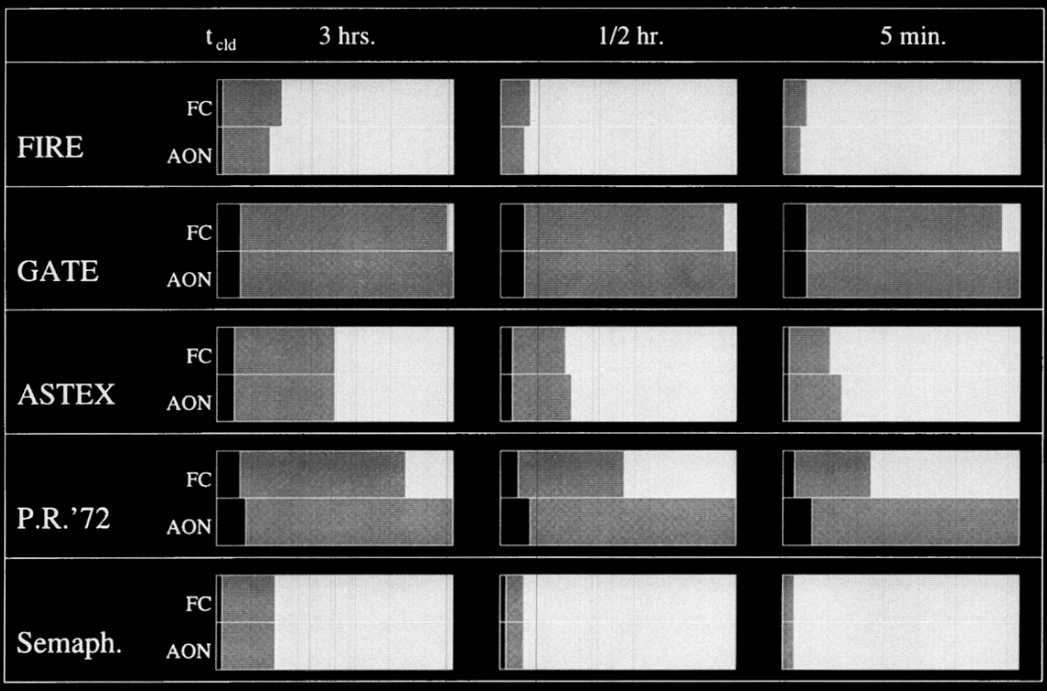

Fig. 7. FC and AON loss rates of SO_2 for the 5 (fractional) cloud cases for the k_l base case and t_{cld} values of 3 h, 30 min, and 5 min, respectively. The loss rates (rounded to units of 2.5%) are pictured proportionally to the production of SO_2. Gas-phase oxidation (white bar), deposition (light-grey bar) and aqueous-phase oxidation (dark-grey bar).

trations in a fractional cloudiness MBL deviate between 100% and −100% from those in an all-or-nothing MBL. These values have been found applying a typical range for the mean total water content $\bar{q}_w$ and the variance, σ_s, of q_w and θ_l. We performed simulations for 3 different time scales of exchange between the cloudy and non-cloudy air and three different cloudwater pH values. For 5 different observed (fractional) cloud cases (GATE, Puerto Rico '72, ASTEX, FIRE and Semamphore) SO_2 deviations were found to range between 33% and −85%. In these cases $\bar{q}_w$ and σ_s were determined by the observations. Critical parameters to ΔSO_2 are the time scale of exchange between cloudy and non-cloudy air, the chemical lifetime of SO_2 in the cloud and the (fractional) cloud cover. Although this investigation has more the character of a sensitivity analysis, we can conclude that application of cloud chemistry in meteorological chemical mesoscale models which take fractional cloudiness into account in the simulation of cloud chemistry will give an important improvement of the quantification of the different formation and loss pathways of sulfur. Meanwhile, in absence of a feasable way to implement gas- and aqueous-phase chemistry in these models, we suggest to use the AON approach but to apply a correction factor. Such a correction factor should account for the differences in SO_2 oxidation in the presence of fractional cloudiness and may be derived from off-line calculations similar to those performed in this study.

6. Acknowledgements

The authors thank Jordi Vilà-Guerau de Arellano and three anonymous reviewers for helpful comments on the manuscript. The first author has been funded by the CEE through the program Human Capital and Mobility (contract no. ERBCHBG CT 93-0349). This work has been partially funded by the CNRS atmospheric chemistry program, PNCA. Computing resources have been made available by CNRS-IDRIS.

REFERENCES

Albrecht, B. A., Jensen, M. P. and Syrett, W. J. 1995. Marine boundary layer structure and fractional cloudiness. *J. Geophys. Res.* **100**, 14 209–14 222.

Albrecht, B. A., Randall, D. A. and Nicholls, S. 1988. Observations of marine stratocumulus clouds during FIRE. *Bull. Amer. Meteor. Soc.* **69**, 618–626.

Andreae, O. M. and Raemdonck, H. 1983. Dimethyl sulfide in the surface ocean and the marine atmosphere, global view. *Science* **211**, 744–747.

Bechtold, P., Fravalo, C. and Pinty, J. P. 1992. A model of marine boundary-layer cloudiness for mesoscale applications. *J. Atmos. Sci.* **49**, 1723–1744.

Bechtold, P., Pinty, J. P. and Mascart, P. 1993. The use of partial cloudiness in a warm-rain parameterization: a subgrid-scale precipitation scheme. *Mon. Wea. Rev.* **121**, 3301–3311.

Berge, E. 1993. Coupling of wet scavenging of sulphur to clouds in a numerical weather prediction model. *Tellus* **45B**, 1–22.

Brümmer, B. 1978. Mass and energy budgets of a 1 km high atmospheric box over the GATE C-scale triangle during undisturbed and disturbed weather conditions. *J. Atmos. Sci.* **35**, 997–1011.

Cahalan, R. F., Silberstein, D. and Coakley, J. A. 1995. Liquid water path and plane-parallel albedo bias during ASTEX. *J. Atmos. Sci.* **52**, 3002–3012.

Calvert, J. G. and Stockwell, W. R. 1984. The mechanisms and rates of the gas phase oxidations for sulfur dioxide and nitrogen oxides in the atmosphere. In: J. G. Calvert (ed.): *SO_2, NO and NO_2 oxidation mechanisms: atmospheric considerations*, Butterworth, Boston, 1–62.

Chang, F-L. and Coakley, J. A. 1993. Estimating errors in fractional cloud cover obtained with infrared threshold methods. *J. Geophys. Res.* **98**, 8825–8839.

Cuijpers, J. W. M. and Bechtold, P. 1995. A simple parameterization of cloud water related variables for use in boundary layer models. *J. Atmos. Sci.* **52**, 2486–2490.

Daum, P. H. 1990. Observations of H_2O_2 and S(IV) in air, cloudwater and precipitation and their implications for the reactive scavenging of SO_2. *Atmos. Res.* **25**, 89–102.

Eymard, L., Planton, S., Durand, P., Camus, Y., Le Traon, P. Y., Prieur, L., Weill, A., Hauser, D., Le Squere, B., Rolland, J., Pelon, J., Baudin, F., Benech, B., Brenguier, J. L., Caniaux, G., de Mey, P., Dombrowski, E., Druilhet, A., Dupuis, H., Ferret, B., Flamant, C., Flamant, P., Hernandez, F., Jourdan, D., Katsaros, K., Lambert, D., Lefevre, J. M., Le Borgne, P., Marsoin, A., Tournadre, J., Trouillet, V. and Zakardjian, B. 1996. Study of the air-sea interactions at the mesoscale: the SEMAPHORE experiment. *Ann. Geophys.*, in press.

Hahn, C. J., Warren, S. G., London, J., Chervin, R. M. and Jenne, R. 1982. *Atlas of simultaneous occurrence of different cloud types over the oceans.* NCAR Technical Note TN-201+STR, Boulder, Co.

Hynes, A. J., Wine, P. J. and Semmes, D. H. 1986. Kinetics and mechanism of OH reactions with organic sulfides. *J. Phys. Chem.* **90**, 4148–4156.

Iribarne, J. V. and Cho, H. R. 1989. Models of cloud chemistry. *Tellus* **41B**, 2–23.

Jacob, D. J. 1986. Chemistry of OH in remote clouds and its role in the production of formic acid and peroxymonosulfate. *J. Geophys. Res.* **91**, 9807–9826.

Johnson, D. W., Martin, G. M., Taylor, J. and Gibbs, M. 1993. *ASTEX flight summary for U. K. C-130, report.* Meteorol. Res. Flight, Cardington, England.

Karamchandani, P. and Venkatram, A. 1992. The role of non-precipitating clouds in producing ambient sulfate during summer: results from simulations with the acid deposition and oxidant model (ADOM). *Atmos. Environ.* **26A**, 1041–1052.

Krueger, S. K., McLean, G. T. and Fu, Q. 1995. Numerical simulation of the stratus-to-cumulus transition in the subtropical marine boundary layer. Part II. Boundary-layer circulation. *J. Atmos. Sci.* **52**, 2851–2868.

Lelieveld, J. and Crutzen, P. J. 1990. The influences of cloud photochemical processes on tropospheric ozone. *Nature* **343**, 227–233.

Lelieveld, J. and Crutzen, P. J. 1991. The role of clouds in tropospheric photochemistry. *J. Atmos. Chem.* **12**, 229–267.

Matthijsen, J., Builtjes, P. J. H. and Sedlak, D. L. 1995. Cloud model experiments of the effect of iron and copper on tropospheric ozone under marine and continental conditions. *Meteor. Atmos. Phys.* **57**, 43–60.

McHenry, J. N. and Dennis, R. L. 1994. The relative importance of oxidation pathways and clouds to atmospheric ambient sulfate production as predicted by the regional acid deposition model. *J. Appl. Meteor.* **33**, 890–905.

Mocko, D. M. and Cotton, W. R. 1995. Evaluation of fractional cloudiness parameterizations for use in mesoscale models. *J. Atmos. Sci.* **52**, 2884–2901.

Müller, F., Clappier, A. and Krüger, B. 1996. On the consideration of clouds in Eulerian chemistry transport models. *Proceedings of EUROTRAC symposium '96*, P. M. Borrel, P. Borrel, T. Cvitas, K. Kelly and W. Seiler (eds.): Computational mechanics publication, Southampton.

Nguyen, B. C., Bonsang, B. and Gaudry, A. 1983. The rôle of the ocean in the global atmospheric sulfur cycle. *J. Geophys. Res.* **88**, 10903–10914.

Pennel, W. T. and LeMone, M. A. 1974. An experimental study of turbulence structure in the fair-weather trade wind boundary layer. *J. Atmos. Sci.* **31**, 1308–1323.

Schwartz, S. E. and Freiberg, J. E. 1981. Mass-transport limitation to the rate of reaction of gases in liquid-water clouds. In: W. Jaeschke, (ed.): *Chemistry of multi-*

phase systems, G6. Springer Verlag, New-York, 415–471.

Schwartz, S. E. 1994. Cloud studies seen from a physical chemist's perspective. In: G. Angeletti and G. Restelli (eds): *Physico-chemical behaviour of atmospheric pollutants*. 2. Proc. of the 6th European Symp., Varese, Italy, 1993. Report EUR 15609/2 EN, 891–900.

Sedlak, D. L. and Hoigné, J. 1994. The Oxidation of S(IV) in Atmospheric Water by Photooxidants and Iron in the Presence of Copper. *Environ. Sci. Technol.* **28**, 1898–1906.

Sievering, H., Boatman, J., Luria, M. and van Valin, C. C. 1989. Sulfur dry deposition over the western North Atlantic: the rôle of coarse aerosol particles. *Tellus* **41B**, 338–343.

Sievering, H., Boatman, J., Gorman, E., Kim, Y., Anderson, L., Ennis, G., Luria, M. and Pandis, S. 1992. Removal of sulphur from the marine boundary layer by ozone oxidation in sea-salt aerosols. *Nature* **360**, 571–573.

Shi, B. and Seinfeld, J. H. 1991. On mass transport limitation to the rate of reaction of gases in liquid droplets. *Atmos. Environ.* **25A**, 2371–2383.

Suhre, K. and Rosset, R. 1994. DMS oxidation and turbulent transport in the marine boundary layer: a numerical study. *J. Atmos. Chem.* **18**, 379–395.

Thompson, A. M. 1995. Measuring and modeling the tropospheric hydroxyl radical (OH). *J. Atmos. Sci.* **52**, 3315–3327.

Twohy, C. H., Austin, P. H. and Charlson, R. J. 1989. Chemical consequences of the initial growth of cloud droplets: a clean marine case. *Tellus* **41B**, 51–60.

Warneck, P. 1988. Chemistry of the natural atmosphere. *Int. Geophysics Series* **41**, Academic Press, New York.

Warren, S. G., Hahn, C. J., London, J., Chervin, R. M. and Jenne, R. L. 1988. *Global distribution of total cloud cover and cloud type amounts over the ocean*. NCAR Technical Note TN-317+STR, Boulder, Co.